Delay induced double explosive transition in a swarmalator system

Carmel T. Lambu,[1,2,*] Romuald T. Mbonwouo,[1,2] Gael R. Simo,[2,3] Delors A. Jiofack,[2,4] Steve J. Kongni,[1,2,†] Patrick Louodop,[1,2,5,6] and Hilda A. Cerdeira[7]

[1]*Research Unit Condensed Matter, Electronics and Signal Processing, University of Dschang, P.O. Box 67, Dschang, Cameroon*
[2]*MoCLiS Research Group, Dschang, Cameroon*
[3]*Laboratory of Electrotechnics, Automatics and Energy, Department of Maintenance, Higher Technical Teachers, Training College (HTTC) of Ebolowa, University of Ebolowa, Cameroon*
[4]*Department of Physics - FFCLRP, University of São Paulo (USP), 14040-901 Ribeirão Preto - SP, Brazil*
[5]*ICTP South American Institute for Fundamental Research, São Paulo State University (UNESP), Instituto de Física Teórica, Rua Dr. Bento Teobaldo Ferraz 271, Bloco II, Barra Funda, 01140-070 São Paulo, Brazil*
[6]*Potsdam Institute for Climate Impact Research (PIK), Member of the Leibniz Association, P.O. Box 60 12 03, D-14412 Potsdam, Germany*
[7]*São Paulo State University (UNESP), Instituto de Física Teórica, Rua Dr. Bento Teobaldo Ferraz 271, Bloco II, Barra Funda, 01140-070 São Paulo, Brazil and Epistemic, Gomez & Gomez Ltda. ME, Rua Paulo Franco 520, Vila Leopoldina, 05305-031 São Paulo, Brazil*

(Received 26 May 2025; accepted 19 December 2025; published 4 February 2026)

Synchronization and aggregation are important phenomena in the world, and many systems exhibit them. The swarmalator system is a good example, arousing interest from many scientists recently. Despite its rising interest, many do not consider delay of any form. Knowing that delay makes the system more realistic, surely containing rich dynamics, we use a delay term in the internal phase dynamics. Spanning through the various parameters and domains of this model, with the order parameter in its local and complex form, shows very interesting dynamics like the boiling chimera state in various domains and the ring static sync, which are primer discoveries in the field of delayed swarmalators. Also, the existence of phase delay helps us highlight a double explosive transition—first from synchronous to asynchronous and, secondly, from asynchronous to synchronous states, which have been used to understand some brain diseases. In this study, we lay down an additional base to the understanding of delay where environmental factors account for it, and so, we pave the way for more studies considering the reality of the environment on mathematical models.

DOI: 10.1103/hhzm-zfxt

I. INTRODUCTION

The study and understanding of collective behavior continue to attract the attention of scientists since the behaviors observed in such studies have applications in many areas of life [1–3] such as the flight of birds [4], spermatozoa dynamics [5], schools of fish [6] or even the movement of sheep [7]. The study of collective movements, in general, is an important asset for understanding and reproducing living phenomena on an industrial scale.

To achieve this, several models have been developed to explain certain natural behaviors. However, among the models proposed over the centuries, the focus has been on systems that can highlight synchronized states, clusters, chimera states, and more while remaining static in a given space. This type of system, known as an *oscillator* [8,9], quickly showed its limitations when it came to understanding the movements of living entities capable of moving in space. To overcome this, the modeling of mobile oscillator systems as proposed by Vicsek *et al.* [10] and later by Sun *et al.* [11] has made it possible to highlight aggregation. To establish a link between synchronization (temporal self-organization) and aggregation (spatial self-organization), O'Keeffe *et al.* [12] defined a model of systems which they called *swarmalator*, in which the internal dynamics of an entity influences that of the external. Based on their model, several investigations have been carried out that have led to better understanding of the dynamics of mobile systems and are still sources of questioning and investigation, both for pairwise interaction [12–18] as well as higher-order interactions [19] whose applications can be found in the field of robotics [20–23] and in small organisms such as tree frogs that understand synchronization in their vocal rhythms [24].

Synchronization in this field is a recurrent word and involves two main types of transitions, which are first- and second-order phase transitions to synchronization. Rosenblum *et al.* [25] investigated the behavior of a system of identical oscillators that were coupled through a small number of links, and their discovery suggested that a critical phenomenon could occur. However, the first-order or explosive synchronization was highlighted by Gómez-Gardeñes *et al.* [26] providing explanations for microscopic critical phenomena. They found that the oscillators could suddenly synchronize,

*Contact author: lambucarmel@gmail.com
†Contact author: kongnisteve@yahoo.fr

even when the coupling strength was weak. Explosive synchronization is a phenomenon that has been observed in various configurations in dynamical systems [11,27–29].

Again, exploring the dynamics of a multiplex of Kuramoto systems, Wu *et al.* [30] showed the existence of a double explosive transition from a synchronous to an asynchronous state and vice versa, like that of Hong [31] who investigated the behavior of a system of coupled Kuramoto oscillators under attractive and repulsive forces. They found that this system could exhibit explosive synchronization when the coupling strength was sufficiently strong. This phase transition occurs when a group of oscillators that are initially out of phase suddenly synchronize, and this is often due to a change in the state of the system due to some of its parameters. More light was shed on explosive synchronization in collective motion studies, when it was discovered by a team of scientists working on a multiplex of systems of swarmalators under the effect of interlayer attractive and repulsive coupling [17]. Recently, it was also shown that even higher-order interactions can give way to abrupt transitions in swarmalator systems [19].

For a system of interacting elements, the environment in which they are found can affect the way they interact, more specifically, their synchronization and aggregation. To cater for this, scientists usually introduce the notion of delay, which makes the system one step closer to reality and, in the same line, the observable outcomes [11,32–34]. Recently, Blum *et al.* [32] introduced delay in a system of swarmalators (self-propelling particles that interact with each other through a combination of attractive and repulsive forces), and this was mainly on the internal phase dynamics, thus giving birth to additional dynamics. They limited themselves to the active phase wave domain and to the characterization of these dynamics.

In this paper, we will explore the concept of phase transitions in delayed swarmalators and its potential applications in various fields crossing over through dynamics observed in other domains than the active phase wave domain. We observe that there is a recurring first-order phase transition upon varying the coupling strength and some additional dynamics like the concentric cluster, static sync, and a chimeralike state originating from the boiling state (BS) discovered by Blum *et al.* [32]. These studies suggest that explosive synchronization is a phenomenon that can occur in a wide range of self-organizing systems, including swarmalators. The ability of these systems to suddenly synchronize in response to small perturbations has important implications for the development of technologies, including robotics and autonomous vehicles.

This paper is made up of four sections structured as follows. In Sec. II, we present the model of our study and the various parameters of interest. We also list the various analytical tools of importance to our study. In Sec. III, we bring in the comparison between synchronization transitions in the absence of delay and in its presence in all these under numerical solutions. In Sec. IV, we present brief conclusions. To support some results, we have provided movies in [35] and figures in the Supplemental Material [36].

II. DELAY MODEL

In this model, the swarmalator is represented by two parts: an agent, whose spatial dynamics is described by X_k, and an internal oscillator described by a phase θ_k. These two elements interact as introduced in the model proposed in Refs. [12,13]. By considering the delay in the internal dynamics, the study model can be written as follows [32]:

$$\dot{X}_k = v_k + \frac{1}{N}\sum_{j\neq k}^{N}\left\{\frac{X_{jk}}{\|X_{jk}\|}[A + J\cos(\theta_{j\tau} - \theta_k)] - B\frac{X_{jk}}{\|X_{jk}\|^2}\right\}, \tag{1}$$

$$\dot{\theta}_k = w_k + \frac{K}{N}\sum_{j\neq k}^{N}\frac{\sin(\theta_{j\tau} - \theta_k)}{\|X_{jk}\|}, \tag{2}$$

for $j = 1, \ldots, N$, where N represents the population size, $X_k = (x_{1k}, x_{2k})$ is the position, and θ_k is the internal phase of the kth swarmalator. Here, v_k is the natural velocity, which is also the spatial velocity of each swarmalator at the onset of the study, and ω_k is the corresponding natural frequency of each oscillator. In Eqs. (1) and (2), A and B are constant ($A = B = 1$), where A ensures the particles do not dissipate forever, while B ensures that the swarmalators do not aggregate into a single point, and there is no delay in the space variable. Here, $\theta_{j\tau}$ is the contracted form of $\theta_j(t - \tau)$ and θ_j that of $\theta_j(t)$. This is the same for X_k, which is the contracted form of $X_k(t)$. Here, X_{jk} is equivalent to $X_k - X_j$.

The system in Eqs. (1) and (2) is governed by three main parameters which are J, K, and τ. Here, K is a constant which, when multiplied by $1/||X_{jk}|| = 1/||X_k - X_j||$, represents the phase coupling strength between the phases of the internal dynamics.

The interaction between the space and the phase dynamics is modulated by the term $A + J\cos(\theta_{j\tau} - \theta_k)$. Here, J ($\in [-1, 1]$) is the coefficient that enables, depending on its value, whether there can be attraction or repulsion between entities by being positive or negative. For simplicity, we choose identical swarmalators $v_k = v$ and $\omega_k = \omega$, and for this system, we take v and ω equal to zero. A particle at time t responds to the phase of another particle j at time $t - \tau$.

Five main spatial configurations were initially found as a function of the pair (J, K) [12,14] in the absence of delay. Many other patterns have been observed upon trying to show the influence of the coupling parameter on the aggregation and synchronization of swarmalators. Kongni *et al.* [17] showed the appearance of two additional states before synchronization occurs. Jiménez-Morales [37] and Sar *et al.* [14] studied the competitive behavior between the positive and negative values of the phase coupling, showing that this system can have a dynamically synchronized or asynchronous state and many other configurations due to the form of the repulsive interaction term. According to this description, the authors showed that we can have mixed patterns, clusters, and synchronization.

In this study, we will consider coupled identical swarmalators with a delay in their internal phase dynamics. In this paper, we work in various domains of the (J, K, τ) space, mainly pointing out what the outcome in terms of synchronization during phase transitions will be.

Investigating various phase transitions to synchronization in our network will be done in part with the order parameter. For the case of this study, two main order parameters will

be used—one which deals with the internal phase dynamics only (it helps to determine the value of the critical value or minimum value beyond which phase synchronization occurs) and another which helps to bring out the correlation between the internal phase and spatial space dynamics, usually called the *complex order parameter* S [12,13,21,31,37]. The order parameter used by Kuramoto is defined as [8,9] $R\exp(p\Phi) = \frac{1}{N}\sum_{k=1}^{N}\exp(p\theta_k)$, where Φ is the average of the phase of all elements in the network, and $p = \pm\sqrt{-1}$ is an imaginary number. We should take note here that, when the jth and kth particles are synchronized in phase, then the norm R is closer to 1. In the case $R < 1$, there is no phase synchronization.

To measure the correlation between the spatial angle ϕ and the internal phase dynamics θ of the swarmalators, we define the complex order parameter S as follows: $S_{\pm}\exp(p\Psi_{\pm}) = \frac{1}{N}\sum_{i=1}^{N}\exp[p(\phi_i \pm \theta_i)]$, where S is the maximum value between S_+ and S_-. It will imply $S = \max(S_+, S_-)$ is the complex order parameter, and from its analysis, if $S = 1$, there is total correlation between the spatial phase ϕ and the internal phase θ of elements in the network, while if $S \approx 0$, it indicates a lack of correlation. To appreciate and differentiate between the static and active states, we use the mean speed [12,14,17] $V = \frac{1}{N}\sum_{i=1}^{N}\sqrt{(\dot{x}_{1i}^2 + \dot{x}_{2i}^2)}$ [12,14,17].

Coupled to this, we sort the phases in groups, which permit supplementing the undecided zones upon which the order parameters alone could not shed enough light. Unlike other works using the Kuramoto order parameter or the velocity [16,17,32], in this study, we show the limits of these order parameters since differentiating zones of clusters and complete phase synchronization here is difficult with these order parameters.

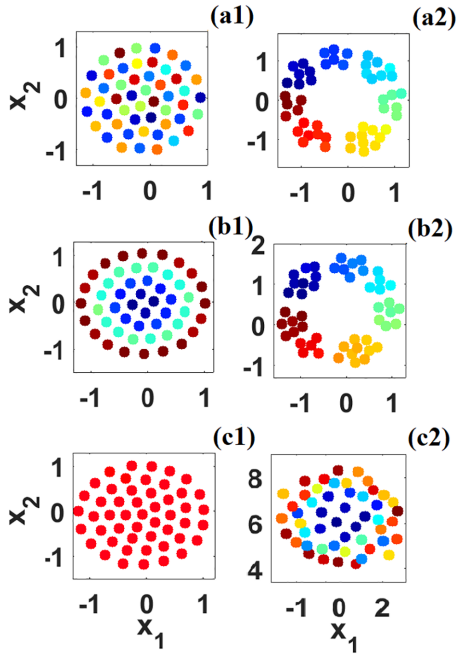

FIG. 1. Spatial pattern formation for $N = 50$ swarmalator dynamics with chosen values in the (J, K, τ) space as the delay increases as $(a_i- > b_i- > c_i)$ [12,13]. Here, (a1) is plotted with $(J, K, \tau) = (0.1, -1, 0)$ for the SA phase and (a2) with $(J, K, \tau) = (1, -0.1, 0)$ for SpPW. Notice that, for the first set of parameters corresponding to the SA phase, while increasing the delay [$\tau = 5$, at (b1)], the system undergoes the transition SA $\rightarrow$ RSS $\rightarrow$ SS. For the second set of parameters starting at the SpPW, the system remains at the same phase for (a2) $\rightarrow$ (b2). Then it transitions to a form of a fast BS [at (c2) for $\tau = 50$] since the external elements form a group of moving elements that enclose a static region (see Movies 1–3 in [35]).

III. NUMERICAL RESULTS

We consider a system of $N = 50$ identical swarmalators. For the numerical integration, the Runge-Kutta fourth-order algorithm was used with a time step $dt = 0.05$, a transient time $t_{\min} = 80\%$ of the final time, such that the total number of iterations is usually 2.10^4, and time 4000 units. Unless the influence of time is desired to extend beyond, we remain within this time unit. The spatial initial conditions were uniformly distributed between $[-1; 1]$ and the phase within $[-\pi; \pi]$.

A. Delayed states

As far as systems of swarmalators are concerned, several dynamics arise when their agents interact. Some of these observed dynamics in the absence of delay include static sync (SS), static async (SA), static phase wave (SPW), splintered phase wave (SpPW), active phase wave (APW), static π (SPI), and the static wing phase wave (SWPW) [12,13,15,17,32,38], and when delay exists, the BS and the pseudochristaline state [quasistatic state (QSS)] [32] have been mentioned. In this work, we will span three main domains of the J-K space, which include the SA, SPW, and SpPW domains, in the presence of delay. The APW domain was studied by Blum *et al.* [32] with no direct emphasis on the transition to synchronization. The SPW domain seems to be invariant under the effect of delay since its dynamics remains unchanged. In the following, we show additional collective states with delay.

In Figs. 1(a1) and 1(a2) (first row), we present two previously known phases SA (column 1) and SpPW (column 2) without delay [5,12–15,32,38]. The second and third rows represent them with delay, where there appears a new phase which will be described shortly [Fig. 1(b1)]. The spatial representation of the swarmalators is shown, while the colors indicate the internal phase dynamics. Figures 1(c1) and 1(c2) in the third row represent scatter plots for strong enough delay with a value of 50. The time evolution of a snapshot of Fig. 1(c2) is seen in Movie 3 in [35]. The triplets values (J, K, τ) on this graph are selected to facilitate the comparison between calculations with and without delay. This figure shows that there are transitions to different states in various domains upon increasing the delay strength. By observing the first column, Figs. 1(a1), 1(b1), and 1(c1), there is a significant change in the static async state when low delay is introduced, as seen in Fig. 1(b1)), forming ring clustered structures, and similar to Fig. 1(c1), forming a static sync structure. It has been shown by Blum *et al.* [32] that the APW contains the BS when low delay values are introduced just above a defined transitional value of delay for a given set of parameters like J, K, τ, and N. In our case, different regions of the parameter space produce different collective states. The

time evolution of Fig. 1(b1) with low delay can be observed in Movies 1 and 2 in [35].

For the SPW, not shown here, where $K = 0$, there is no observable change, be it in weak or strong delay, with the tools at hand. Particularly, the fact that K has a value of zero surely reduces the influence of τ, and hence, the state is seemingly unchanged. We can therefore observe here that, for a weak delay ($\tau = 5$), a system in SA tends to phase synchronize, forming clusters, while one in the SpPW seems to be unchanged under low delay. As observed in Figs. 1(a1), 1(b2), and 1(c2), these states suggest there is a transitional value of delay, to be determined, for which there is a transition from the SpPW observed in zero and weak delay to the BS.

Ring static sync (RSS). When delay is introduced in the SA state, we obtain a new state which we call the ring static sync (RSS), Fig. 1(b1). An appearance in the literature of a similar state for a different model is that of Hindes *et al.* [39]. Ring states or ring waves were also reported in Refs. [15,37] where a ring wave is a mixture of many phases. This state is similar (having rings) but different from our case, where each ring has a single phase value, and the phase difference between consecutive rings is close to 2π. We call this state RSS because it forms clustered rings, and it appears to be static; its velocity is very close to zero. It arises when delay is introduced in a no-delay SA state, and the elements are seen to reorganize into clusters when delay reaches a certain value.

Boiling state (BS). As discovered by Blum *et al.* [32], this state was encountered in a delayed swarmalator system in the APW domain [32]. Its characteristic features are its static internal elements and its boiling external agents, showing clearly where its name comes from. During this study, we noticed that, for a small number of node agents, and in the SpPW domain with sufficient delay above the transition value of delay (observed with the order parameter), a BS appears, as seen in Movie 3 in [35] ($N = 50$), which seems to be a disordered state but with a greater number of particles; it is more visible. Their time evolution is shown in Movie 4 in [35] with a greater number of nodes ($N = 600$), where the BS appears after a transient of 350 unit times. Also, the internal radius of static elements was seen to depend on the K values, such that the smaller $|K|$, the smaller this radius, and it also depends on the number of nodes in the system. It is important to lay down these characteristics to permit us to differentiate the BS in Figs. 2(a) and 2(c) from the one observed in this article and shown in Figs. 2(b) and 2(d) and defined as follows.

Boiling chimera state (BCS). This additional state, which we shall call the boiling chimera state (BCS), is observed to have an internal single-phase state surrounded by clustered phase rings, see Fig. 2(d). While at first sight BS and BCS appear as very similar in a static picture [Figs. 2(c) and 2(d)], Movies 4 and 5 in [35] show that the internal phase synchronized state is stable in the BS case and changes periodically in the BCS. It is also interesting to notice the distribution of phases in Figs. 2(a) and 2(b); BS presents all phases more or less localized while they are separated by 2π, and BCS has an internal synchronized cluster and most phases randomly distributed, as described in the next paragraph.

The internal dynamics organization is key to differentiate the BS from the BCS. Even when both states appear to be similar, the inner part of the BS presents some clusters of the internal phase, while in the BCS, all internal elements are phase synchronized, as can be seen in Figs. 3(a) and 3(b), respectively, keeping the same colors as those of Fig. 2. We observe that the BS is characterized by the formation of identified clusters, where each cluster is separated from the others by a phase difference of 2π.

In contrast with Fig. 3(a), Fig. 3(b) shows the phase snapshot of the elements obtained in the BCS. Here, we can see two main groups: a desynchronized group and, at the top, a quasisynchronized group (characterized by brown coloring), as previously described in Fig. 2(b). From this, we can conclude that the BS observed by Blum *et al.* [32] corresponds to the formation of spatial clusters without perfect coexistence of order and disorder. Unlike the BS, the BCS reveals the coexistence of coherence and incoherence among the phases of the entities, which aligns with the definition of a chimera state [40–42].

The dependence on the number of nodes during a transition is of prime importance since it gives us information on what is happening within the system. In the BCS represented in red in Fig. 4, there is no dependence on the number of nodes for the delay at the transition to synchronization (τ_T). This is to say that, no matter the number of elements in the system, the transition basically occurs around the same value of delay. This value is shown with a horizontal line around the value of $\tau = 2$ [see that the BCS phase appears only around $\tau = 2$, Figs. 5(a) and 5(b)]. Here, we should note that the delay value of transition refers to the value beyond which the order parameter $R = 1$ and below which the order parameter $R \neq 1$. From Blum *et al.* [32], below the curve for these transitional values of delay (from $\tau = 5$ upward), as seen in red in Fig. 4, we have the BS, and above, we have the QSS. We should note that this happens for very specific parameters in the (J, K) space.

The impact of the phase delay, in addition to the BSs, has highlighted other states which, in light of the work on which we rely, have not yet been observed. Thus, to analyze the transition toward phase synchronization, we have represented in Fig. 5 the influence of delay on these transitions for different pairs of the (J, K) space. These figures illustrate the evolution of the order parameters R, S, and the average velocity V of the entities, shown respectively in blue, black, and red, as a function of the delay τ, which varies within the interval $[0, 4.5]$. The phases, identified visually, are shown in each region.

For a phase coupling of $K = -1$ and for three values of the spatial coupling $J = -1$, 0.1, and 1 [corresponding, respectively, to Figs. 5(a)–5(c)], it is observed that increasing the delay tends to lead the elements toward a RSS state, which corresponds to the state shown in Fig. 1(b1). This state is particularly characterized by a phase difference of 2π between rings of identical phase. In Figs. 5(a) and 5(b), one can see that the transition to the RSS state passes through the SA state and BCS. A negative spatial coupling $J = -1$ promotes the clustering of entities with identical phases, with $S \approx 1$ for $\tau > 2.5$. For values of $K = -1$ and $J = 0.1$, which favor the formation of the SA state, the existence of a phase delay can alter this behavior, giving rise to BCS and RSS state. Unlike the effect of a negative coupling $J < 0$, positive values

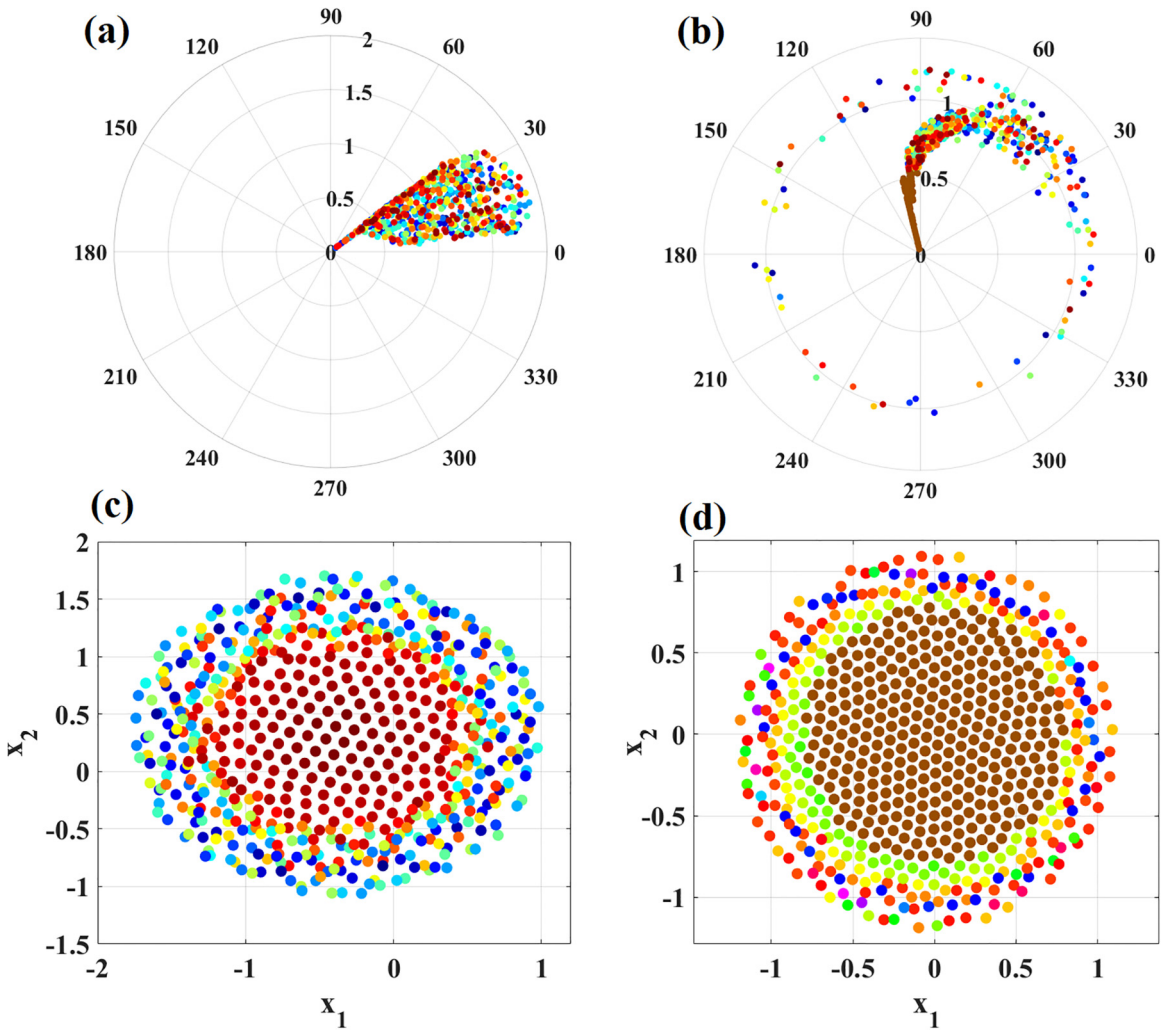

FIG. 2. Snapshot of the internal and external dynamics of $N = 600$ nodes. (a) and (c) BS for $J = 1$ and $K = -0.85$, with delay value of $\tau = 2.05$. (b) and (d) BCS for $J = 0.1$ and $K = -1$, with $\tau = 1.9$. The first row is the polar representation of the internal dynamics θ respecting the distance of each element from the center, and the second row is the scatter plot of the spatial dynamics, where the color represents the internal dynamics (see Movies 4 and 5 in [35]).

$J = 0.1$ and 1 [Figs. 5(b) and 5(c), respectively] lack this clustering ($S \approx 0$) for $\tau > 2$.

Moreover, considering $K = 0.1$, as shown in Figs. 5(d)–5(f), we observe the dominance of the SA state and the absence of a transition to a synchronous state for low ($J = 0.1$) and negative ($J = -1$) values of the spatial coupling [Figs. 5(d) and 5(e)]. However, the emergence of a transition appears as the coupling J increases ($J = 1$), as shown in Fig. 5(f). It can also be noted here that, for $R = 1$, a characteristic of full phase synchronization is biased in this case by the introduction of phase delay, which for high values around $\tau = 15$ reveals the presence of the BS instead of the RSS. In contrast with $K = -1$, for a phase coupling strength of $K = -0.1$, the value of $R = 1$ no longer corresponds to the RSS state but instead signifies the emergence of the synchronization pattern known as the BS, which still appears at larger delay values.

Finally, for $K = 1$ [Figs. 5(g)–5(i)], there is a persistence of the synchronized state characterized by $R = 1$, $S \approx 0$, and $V \approx 0$, regardless of the value of the spatial coupling J or the phase delay τ. This classical form of synchronization is commonly referred to as SS. Based on this analysis shown in Fig. 5, the remaining question concerns the impact of phase delay on the close interplay between spatial and phase coupling strengths.

B. Transition to phase synchronization: Double explosive synchronization

According to the attractive and repulsive interactions that characterize the swarmalator system, the chosen value of the spatial coupling J can help us to show the effect of these interactions on the kind of phase transition to synchronization. This analysis was done in Ref. [17], where they showed the existence of second- and first-order phase transitions to synchronization due to the attractive and repulsive couplings in swarmalator system without the effect of phase delay. In the case of this study, the choice of most spatial coupling values J

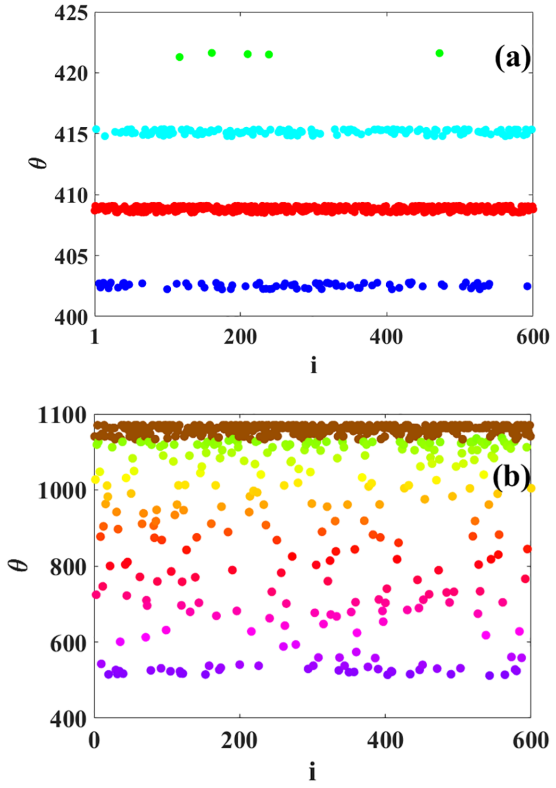

FIG. 3. Snapshots of the internal phase dynamics of each node. (a) BS for $J = 1$ and $K = -0.85$, with $\tau = 2.05$. (b) BCS for $J = 0.1$ and $K = -1$, with $\tau = 1.9$.

led to the formation of double explosive synchronization when varying the phase coupling K for a low value of phase delay $\tau = 4.5$, as shown by Fig. 6(a). As described in Ref.[30], the double explosive synchronization has been observed in a multiplex of Kuramoto systems. This phenomenon can be used to describe the dynamics and functioning of brain diseases [30].

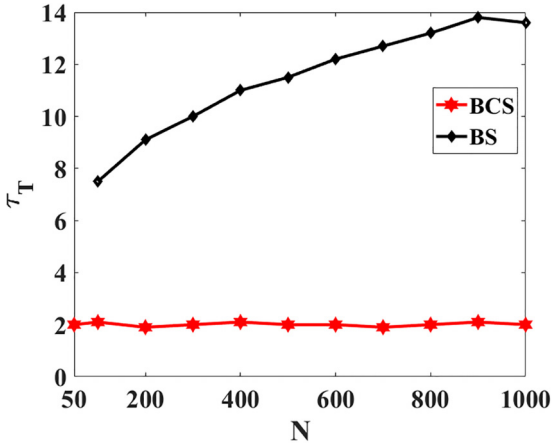

FIG. 4. Dependence of the delay at the transition to synchronization on the system size. Here $(J, K) = (1, -0.7)$ for the black (BS) and $(J, K) = (0.1, -1)$ in red. The data were collected long after the initial conditions and permit us to differentiate between the BCS and the BS.

Figure 6 shows that increasing J for a particular value of delay while varying K leads to a reduction in the gap between the double explosive curves (U-shaped transition), as seen in Fig. 6(a).

It is interesting to observe again the impact that the phase delay has on the phase transitions in the systems of swarmalators. Authors of previous studies have revealed that we can have explosive transition in swarmalators only in the range of attractive phase coupling [17,43], whereas due to the existence of the delay, we observe that there are two transitions, from synchronous to asynchronous state first and, secondly, from asynchronous to phase synchronized state, both explosive transitions that we call *U-shaped abrupt transition*.

When observing the plot in Fig. 6(a), we see there is a form of instability in the plot $J = -1$ during the first transition, which appears as a two-step transition from synchronous to asynchronous state. To investigate and ensure that the observed U-shaped transition to synchronization remains independent of the scale of the value of the control parameter K, we increase the number of steps by taking K between -0.677 to -0.6 with a step of $\delta K = 10^{-6}$. This reveals that the observed fluctuations during the first transition when $J = -1$ in Fig. 6(a) (green) are the result of a power-law relationship that exists between the intermittent evolution of the order parameter and the coupling K in that range, as shown in Fig. 6(b). In this figure, n is the number of towers (where, by *towers*, we mean the intervals with constant $R = 1$) and d the width of a tower. What we observe for $J = -1$ works for various negative values of J, though we did not test the whole sample space of J values. For positive values of J, the transition at the forefront of our U-shaped transition, seen in Fig. 6(a) (red and blue), is of first order.

These double transitions appear here at the same critical value K_c when the phase coupling $K > 0$. In contrast, for negative values $K < 0$, the first transition has different critical values of K that increase as J increases, for a constant value of delay ($\tau = 4.5$). The global effect of these two couplings J and K is shown in Fig. 2(a) in the Supplemental Material [36]. To see the effect of the delay on these double abrupt transitions, we show in Fig. 7 the evolution of the order parameter R as a function of K for several values of delay τ (eight values). In this figure, it appears clearly that the choice of the delay also modifies both the critical value K_c at the first transition and the width between the two transitions called a *double transition width* (TW). Indeed, increasing the values of τ, respectively, from 1 to 4.5 with a step of 0.5 (as indicated in Fig. 7) increases the critical value of the first transition as observed previously in the case of different values of the spatial coupling J (Fig. 6).

The study behind the change of critical values of K at the first transition, in Fig. 7, also reveals the existence of a power-law relationship between critical values K_c and τ present in Figs. 8(a) and 8(c). Additionally, this shows the power-law relationship between τ and the TW in Figs. 8(b) and 8(d). The fitted straight line is colored black, and its slope is $\eta_1 = -1.02$ and $\eta_2 = -0.96$, respectively, in Figs. 8(c) and 8(d).

Extending the analysis performed in Fig. 4 to the value τ_T, where the double transition appears (in the case of Fig. 7, for instance), we can conclude that the double explosive phase transition remains when the number of nodes increases

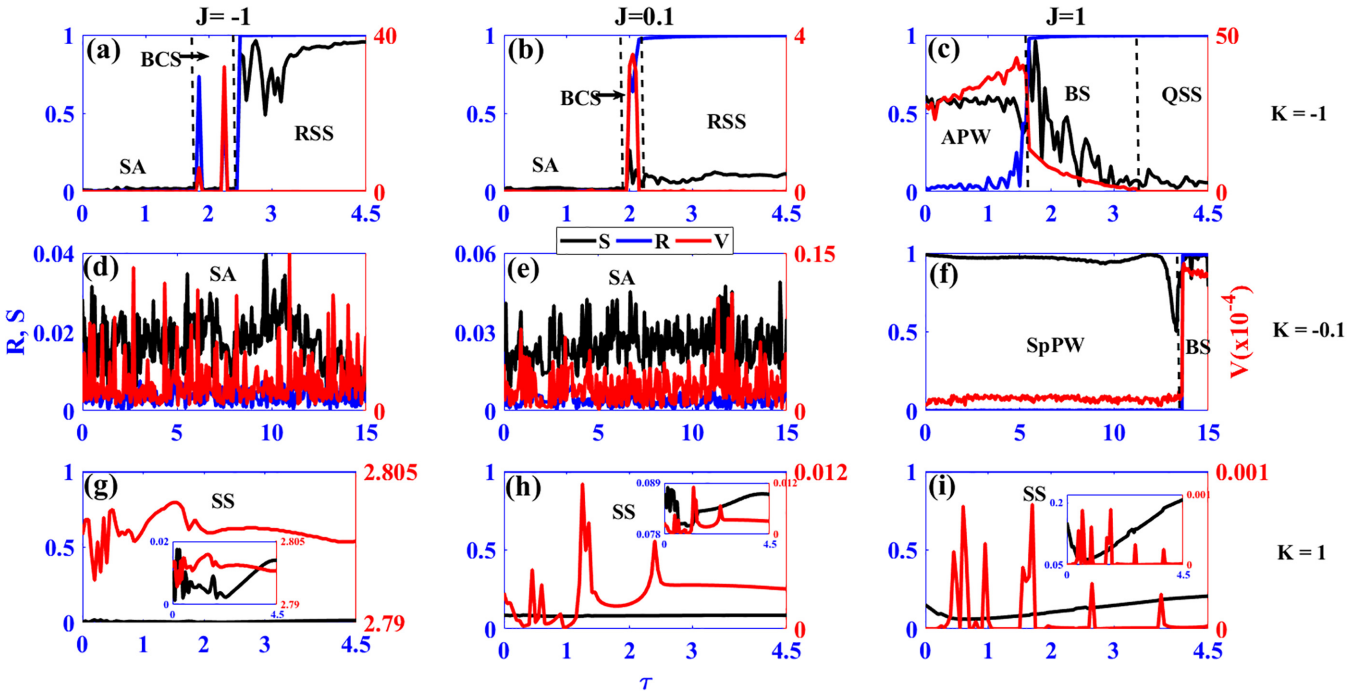

FIG. 5. Order parameters R (blue), correlation S (black) in the right axis, and mean velocity V (red) in the left axis as a function of phase delay τ for different values of the couple (J, K).

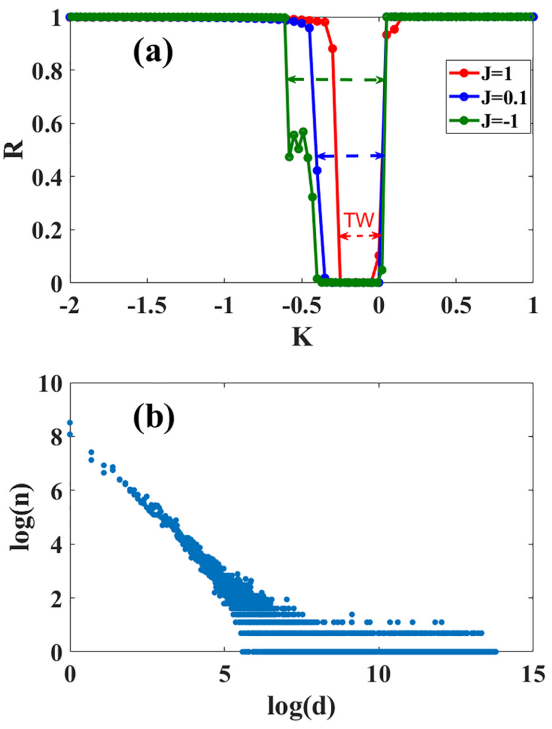

FIG. 6. Influence of the spatial coupling J on the transition to phase synchronization. (a) The mean order parameter R (from 10 initial conditions) as a function of phase coupling K, $-2 < K < 1$, where $J = 1$ (red), $J = 0.1$ (blue), and $J = -1$ (green). (b) Logarithmic plot of the number of towers of height $R = 1$ vs the width of the corresponding towers showing a power-law transition. A tower is defined as an uninterrupted region with $R = 1$.These plots are made for $\tau = 4.5$.

(Fig. 9). Therefore, the size of the network does not affect the appearance of the double explosive transition when $\tau = 4.5$ and $J = 0.1$.We further make a general scan of the (τ, K) space for two values of J with Figs. 10(a) and 10(b) showing the order parameter plots when, respectively, $J = 0.1$ and 1. The light gray color in both with negative values of K indicates a region of cluster states where the phase difference is 2π between two successive clusters. These multicluster states, which normally do not appear in the absence of delay, can be seen in Figs. 10(c) and 10(d) when the delay value is 4.5. Figure 10(f) shows that increasing the delay to a value

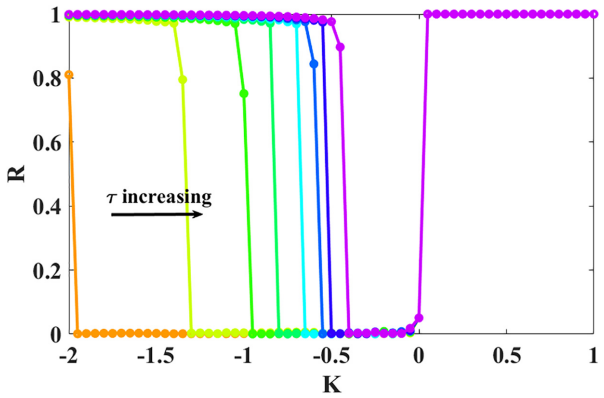

FIG. 7. Double explosive phase transition shown by the order parameter R as a function of the phase coupling strength K for different values of phase delay τ. This shows the effect of phase delay for $\tau = [1; 4.5]$ with a step of 0.5 corresponding, respectively, to each curve from left to right as indicated in the figure. This was plotted for $J = 0.1$ and $\delta K = 0.05$.

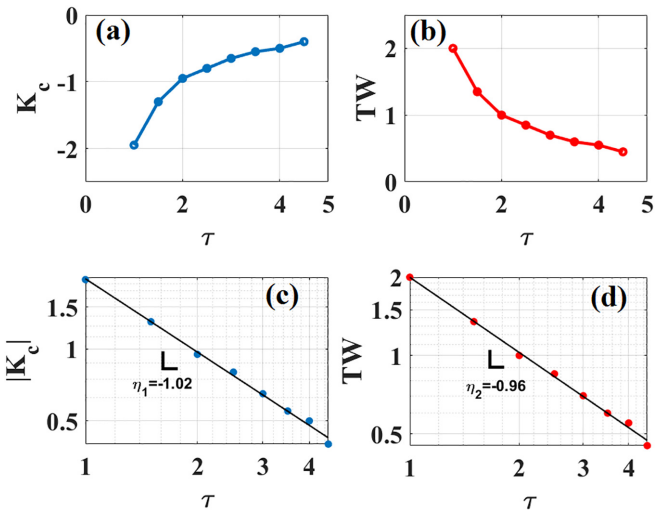

FIG. 8. Power-law evolution induced by the phase delay. (a) and (c) Power-law relationship between K_c and the delay τ. (b) and (d) Power-law relationship between τ and the TW, for $J = 1$ with a critical value at the second transition of $K_{c2} = 0.05$. The TW is defined here by $\mathrm{TW} = |K_{c_2} - K_c|$.

of $\tau = 50$ transforms the disorder state previously present in low delay, as seen in Fig. 10(e) with parameters $(J, \tau, K) = (0.1, 1.95, -0.5)$ to a cluster state with phase difference of 2π between group of elements observed on its time series plot Fig. 10(f)(II).

Similarly, from the region in red (disordered states), the parameter $(J, \tau, K) = (1, 1.95, -0.5)$ given in Fig. 10(j), which is that of a disordered state similar to the APW, will be transformed to a cluster state as observed in Fig. 10(k)(I), more visible with its time series Fig. 10(k)(II), all this when delay is at a value of $\tau = 50$.

When observing Fig. 10(b), the yellow band represents a transition zone from a phase-clustered region to a zone where asynchrony dominates. This leads to Figs. 10(g)–10(i). For Figs. 10(g)(I) and 10(g)(II), we represent a space or scatter plot in Fig. 10(g)(I) and its corresponding time series

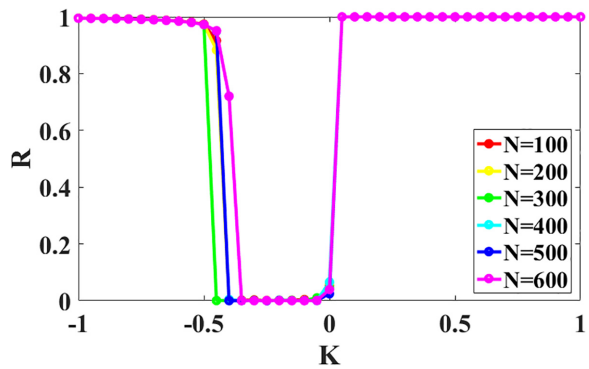

FIG. 9. Size dependence on the existence of the double explosive phase transition. This shows the order parameter R as a function of the phase coupling strength K for a fixed value of phase delay $\tau = 4.5$. This highlights the thermodynamic limit of the explosive transition for the case of $\tau = 4.5$ (violet curve) from Fig. 7 with $J = 0.1$.

in Fig. 10(g)(II) for $N = 600$ elements respecting the same parameters as the simulations to obtain Fig. 10(b), which is for 50 elements at the parameters $(J, \tau, K) = (1, 4.05, -0.4)$. This state is that of a BS with a shorter radius of its quasistatic center. In a similar way, Fig. 10(i) represent a space plot for $N = 600$ elements respecting the same parameters as for the 50 elements in Fig. 10(h) with parameters $(J, \tau, K) = (1, 1.95, -0.85)$ but with a slightly different value of phase delay being $\tau = 2.05$. Though not visible on Fig. 10(h), it corresponds to a BS with 50 elements.

Moreover, the domain of static synchrony seems to remain unchanged, be it with low, see Fig. 10(m), or high values of delay, and this state seems unaffected by the number of elements in the system. Observing Figs. 10(c) and 10(d), these regions appear to have the same order parameter of 1 as in the region of Fig. 10(m). Though they seem to be phase synchronized at the same level as observed with the order parameter having the same color, as in Figs. 10(a) and 10(b), the region in dim white in the negative regions of K and those in the positive domains of K, we can differentiate these two regions using the difference in their phase state values, i.e., 2π. For those in the domain of negative values of K, the phase difference is 2π and is approximately zero for those in the positive region of K. The states of Fig. 10(c) and 10(d) (RSS) have a phase difference of 2π between ring clusters, and those states for a coupling strength $K > 0.1$ have values of approximately 0 (as shown in Fig. 2(b) in the Supplemental Material [36]). More interesting is the behavior of our system for $0 < K \leqslant 0.1$, where we observe a transitional SPI state, Fig. 10(l). Upon increasing the number of nodes while at the same parameters as those for the 50 elements in Fig. 10(l)(II), we observe for the 600 elements in Fig. 10(l)(II) (Movie 6 in [35]) that the same transitory behavior occurs, proving that it is not dependent on the number of nodes. This state is called transitory because, long after the transient time, it forms and later on merges back (disappears), forming the SS state.

IV. CONCLUSIONS

We presented a study of the phase transitions in a time-delayed swarmalator model, and although authors of recent work [11,32] had focused on these systems, we present two additionalstates: the BCS and the RSS. These states are long-time collective states arising due to delay and observed for specific parameters of the (J, K) space in this swarmalator model. It emerges from this study that the introduction of the delay highlights the existence of a double first-order transition. In fact, the transition to reach the synchronization state is characterized by intermediate states such as the BCS and RSS. The BCS is a chimera because, in the scatter plot, we have coherent elements at the center and disordered elements at the exterior, as perceived with the same colors indicating the same phase. What is peculiar is that plotting the phase against the node index, we observe the internal dynamics with some nodes having the same phase and others having different phases [see Fig. 3(b)]. The RSS is called this way because its elements form clusters in a ringlike manner, with each ring having the same phase and thus the same color. We spanned a greater portion of the (J, K) space than Blum *et al.* [32],

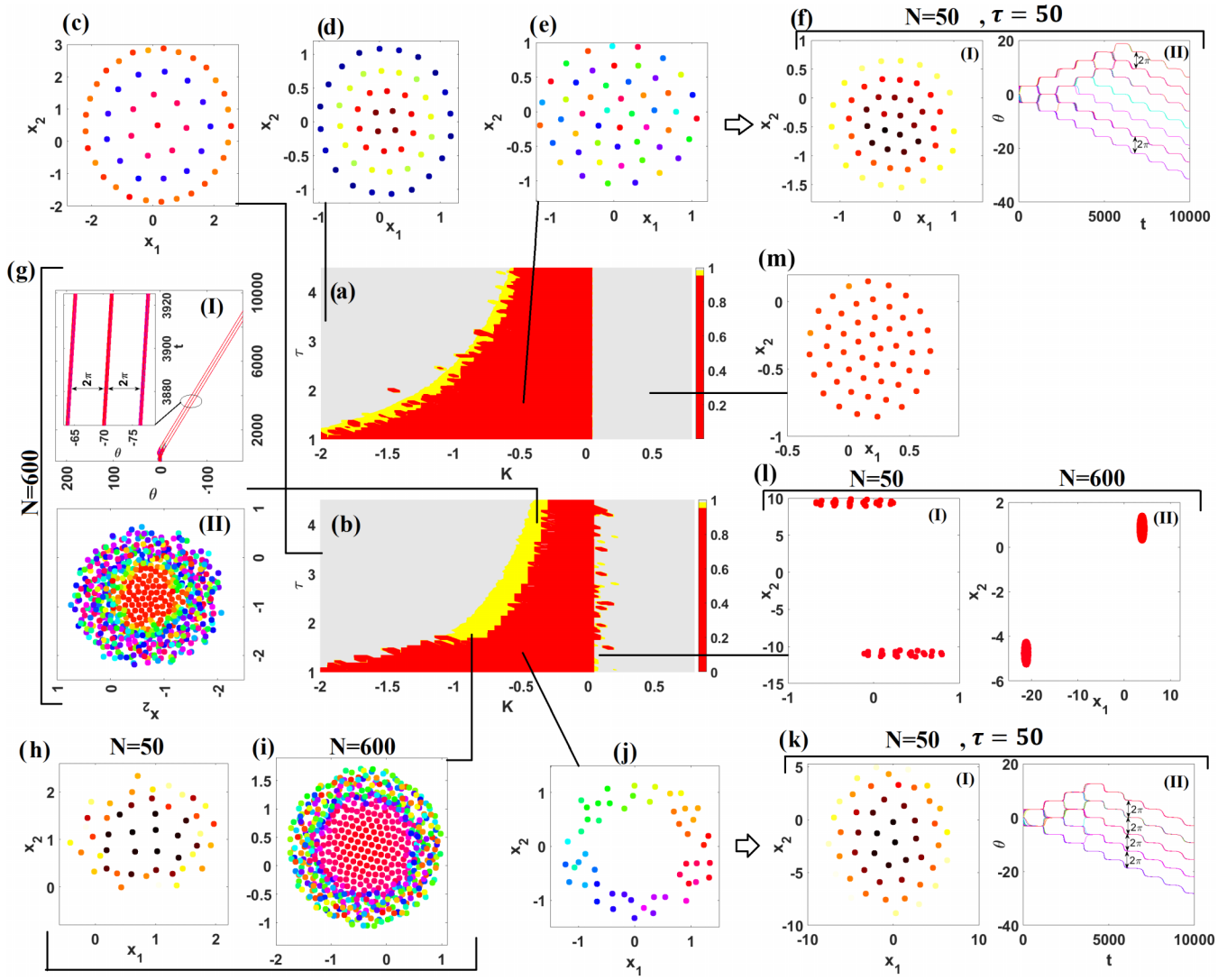

FIG. 10. Collective behaviors of the delayed swarmalator model for τ in the range $1 < K < 4.5$ and the phase coupling K in the range $-2.1 < K < 0.8$. (a) Order parameter plot function of two parameters (τVsK) for $J = 0.1$ and K in the range $-2.1 < K < 0.8$. (b) Order parameter plot function of two parameters (τVsK) for $J = 1$ and K in the range $-2.1 < K < 0.8$. (c) Cluster state for the parameters $(J, \tau, K) = (1, 3.5, -2)$. (d) Cluster state for the parameters $(J, \tau, K) = (0.1, 3.5, -2)$. (e) SA for parameter space $(J, \tau, K) = (0.1, 1.5, -0.5)$. (f) Cluster state for parameter space showing scatter plot with its corresponding time series. (g) BS shown with (I) scatter plot with a small center cluster radius and (II) its corresponding phase-time plot for the parameter space $(J, \tau, K) = (1, 4.05, -0.4)$ using $N = 600$ elements. (h) BS for the parameter space $(J, \tau, K) = (1, 1.95, -0.85)$ using $N = 50$, and (i) BS with a large center cluster radius for the parameter space $(J, \tau, K) = (1, 2.05, -0.85)$ using $N = 600$. (j) APW scatter plot with parameter space $(J, \tau, K) = (1, 1.5, -0.5)$. (k) (I) Cluster scatter plot and (II) its time series with parameter space $(J, \tau, K) = (1, 50, -0.5)$. (l) Snapshot of transitional SPI plots for (I) $N = 50$ and (II) $N = 600$ at $t = 500$ for parameter space $(J, \tau, K) = (1, 1.5, 0.1)$. (m) Scatter plot for SS at the point $(J, \tau, K) = (1, 1.95, 0.5)$.

yet we cannot claim to have uncovered all the rich dynamics that this time-delayed model may contain. Furthermore, it also emerges that, for a specific value of J, for a range of values of K, and for a choice of delay τ, we can observe that the transition to the synchronization state describes a double explosive transition with a U-shape and that the width of this U decreases with increasing delay values, giving rise to a power law. Also, for ranges of values of K and negative values of J, we have zones of intermittence upstream of the beginning of our U-shaped transition where the Kuramoto order parameter R fluctuates mainly between 1 and 0, and this behavior also follows a power law. This type of transition finds applications in the study of brain dynamics, where the first transition can be assimilated to move from the rest phase of the brain to the task phase (the middle portion of our U-shape transition) and the second transition closer to $K = 0$, in our case referring to the onset of an anesthetic-induced unconsciousness, as shown by Tianwei *et al.* [30]. During this study, we observed a limitation using the order parameter (R) because it was unable to differentiate between RSS and SS since RSS contains elements with a difference of 2π between them. This, therefore, calls for us to find other ways to solve this type of problem in the future.

TABLE I. List of dynamical states of swarmalators with and without delay.

No delay	Small delay	Large delay
Static async (SA), O'Keeffe *et al.* [12]	New boiling chimera state (BCS)	New state ring static sync (RSS)
Active phase wave (APW), O'Keeffe *et al.* [12]	Boiling state (BS), Blum *et al.* [32]	Quasistatic state (QSS), Blum *et al.* [32]
Splintered phase wave (SpPW), O'Keeffe *et al.* [12]	SpPW, O'Keeffe *et al.* [12]	BS
Static phase wave (SPW), O'Keeffe *et al.* [12]	Seems unchanged	Seems unchanged
Static sync (SS) state, O'Keeffe *et al.* [12]	Seems unchanged, remaining SS	Seems unchanged, remaining SS

ACKNOWLEDGMENTS

P.L. and H.A.C. are thankful for ICTP-SAIFR and FAPESP Grant No. 2021/14335-0 for partial support. P.L. is grateful for the support of the German Academic Exchange Service (DAAD) for funding his visit at the Potsdam Institute for Climate Impact Research (PIK) under Grant No. (91897150). P.L. thanks Prof. Jürgen Kurths for fruitful discussions. P.L., G.R.S., S.J.K., C.T.L., D.A.J., and MoCLiS research group thank ICTP for the equipment donation under the letter of donation Trieste August 12, 2021.

DATA AVAILABILITY

The data are not publicly available. The data are available from the authors upon reasonable request.

APPENDIX: LIST OF DYNAMICAL STATES OF SWARMALATORS WITH AND WITHOUT DELAY

The number of dynamical states in swarmalator systems is increasing with the zeal and imagination of researchers in the field and at times confusing readers. Here, we present a list of the states known up to today in the hope that it will facilitate search and comparisons. To distinguish the collective behaviors occurring from previous research [12,17,32,44] on swarmalators with this study, we present Table I as a comparison base, restricting ourselves to the O'Keeffe-Hong-Strogatz model [12]. For low and high delay, we refer to Fig. 1, where there is a transitional value of delay for which a change occurs from a said collective behavior. If this transitional value is lacking, then this collective state is said to not be affected by delay.

[1] S. Majhi, B. K. Bera, D. Ghosh, and M. Perc, Phys. Life Rev. **28**, 100 (2019).
[2] T. A. Glaze, S. Lewis, and S. Bahar, Chaos **26**, 083119 (2016).
[3] L. Bauer, J. Bassett, P. Hövel, Y. N. Kyrychko, and K. B. Blyuss, Chaos **27**, 114317 (2017).
[4] D. J. Sumpter, Phil. Trans. R. Soc. B **361**, 5 (2006).
[5] S. Ceron, K. O'Keeffe, and K. Petersen, Nat. Commun. **14**, 940 (2023).
[6] J. de Bie, C. Manes, and P. S. Kemp, Anim. Behav. **167**, 151 (2020).
[7] F. Ginelli, F. Peruani, M. Pillot, H. Chaté, G. Theraulaz, and R. Bon, Proc. Natl. Acad. Sci. USA **112**, 12729 (2015).
[8] Y. Kuramoto and D. Battogtokh, Nonlinear Phenom. Complex Syst. **5**, 380 (2002).
[9] Y. Kuramoto, in *Chemical Oscillations, Waves, and Turbulence* (Springer, Berlin, 1984).
[10] T. Vicsek, A. Czirók, E. Ben-Jacob, I. Cohen, and O. Shochet, Phys. Rev. Lett. **75**, 1226 (1995).
[11] Y. Sun, W. Li, L. Li, G. Wen, S. Azaele, and W. Lin, Phys. Rev. Res. **4**, 033054 (2022).
[12] K. P. O'Keeffe, H. Hong, and S. H. Strogatz, Nat. Commun. **8**, 1504 (2017).
[13] J. U. Lizarraga and M. A. de Aguiar, Chaos **30**, 053112 (2020).
[14] G. K. Sar, S. N. Chowdhury, M. Perc, and D. Ghosh, New J. Phys. **24**, 043004 (2022).
[15] K. P. O'Keeffe, J. H. M. Evers, and T. Kolokolnikov, Phys. Rev. E **98**, 022203 (2018).
[16] H. Hong, K. Yeo, and H. K. Lee, Phys. Rev. E **104**, 044214 (2021).
[17] S. J. Kongni, V. Nguefoue, T. Njougouo, P. Louodop, F. F. Ferreira, R. Tchitnga, and H. A. Cerdeira, Phys. Rev. E **108**, 034303 (2023).
[18] S. J. Kongni, T. Njougouo, G. R. Simo, P. Louodop, R. Tchitnga, and H. A. Cerdeira, in *Artificial Life and Evolutionary Computation* (Springer, Cham, 2025), pp. 223–235.
[19] S. Majhi, M. Perc, and D. Ghosh, J. R. Soc. Interface. **19**, 20220043 (2022).
[20] A. Barciś, M. Barciś, and C. Bettstetter, *2019 International Symposium on Multi-Robot and Multi-Agent Systems (MRS)* (IEEE, Piscataway, NJ, 2019), pp. 98–104.
[21] A. Barciś and C. Bettstetter, IEEE Access **8**, 218752 (2020).
[22] G. Gardi, S. Ceron, W. Wang, K. Petersen, and M. Sitti, Nat. Commun. **13**, 2239 (2022).
[23] Y. Origane and D. Kurabayashi, Symmetry **14**, 1578 (2022).
[24] T. J. Walker, Science **166**, 891 (1969).
[25] M. G. Rosenblum, A. S. Pikovsky, and J. Kurths, Phys. Rev. E **63**, 058201 (2001).
[26] J. Gómez-Gardeñes, S. Gómez, A. Arenas, and Y. Moreno, Phys. Rev. Lett. **106**, 128701 (2011).
[27] S. Boccaletti, J. Kurths, G. Osipov, D. Valladares, and C. Zhou, Phys. Rep. **366**, 1 (2002).
[28] S. Boccaletti, V. Latora, Y. Moreno, M. Chavez, and D. Hwang, Phys. Rep. **424**, 175 (2006).
[29] S. Boccaletti, G. Bianconi, R. Criado, C. I. Del Genio, J. Gómez-Gardenes, M. Romance, I. Sendina-Nadal, Z. Wang, and M. Zanin, Phys. Rep. **544**, 1 (2014).
[30] T. Wu, S. Huo, K. Alfaro-Bittner, S. Boccaletti, and Z. Liu, Phys. Rev. Res. **4**, 033009 (2022).
[31] H. Hong, Chaos **28**, 103112 (2018).

[32] N. Blum, A. Li, K. O'Keeffe, and O. Kogan, Phys. Rev. E **109**, 014205 (2024).
[33] F. M. Atay, Phys. Rev. Lett. **91**, 094101 (2003).
[34] M. Lakshmanan and D. V. Senthilkumar, *Dynamics of Nonlinear Time-Delay Systems* (Springer, Berlin, 2011).
[35] See https://github.com/LATAC-2/Supplemental-movies for the movies of BS, BCS, RSS, SS, and transitional static π.
[36] See Supplemental Material at https://link.aps.org/supplemental/10.1103/hhzm-zfxt for additional figures of the effect of delay on the dynamics.
[37] F. Jiménez-Morales, Phys. Rev. E **101**, 062202 (2020).
[38] K. O'Keeffe and C. Bettstetter, *Micro- and Nanotechnology Sensors, Systems, and Applications XI* (SPIE, Bellingham, 2019), pp. 383–394.
[39] J. Hindes, K. Szwiaykowska, and I. B. Schwartz, Phys. Rev. E **94**, 032306 (2016).
[40] S. Ghosh, S. Pal, G. K. Sar, and D. Ghosh, Phys. Rev. E **109**, 054205 (2024).
[41] G. R. Simo, T. Njougouo, R. Aristides, P. Louodop, R. Tchitnga, and H. A. Cerdeira, Phys. Rev. E **103**, 062304 (2021).
[42] A. Zakharova, *Chimera Patterns in Networks: Interplay between Dynamics, Structure, Noise, and Delay* (Springer, Cham, 2020).
[43] X. Li, P. K. Pal, Y. Lei, D. Ghosh, and M. Small, Phys. Rev. E **111**, 024303 (2025).
[44] S. J. Kongni, T. Njougouo, P. Louodop, R. Tchitnga, F. F. Ferreira, and H. A. Cerdeira, Phys. Rev. E **110**, L062301 (2024).